First-in-human study of AT13148, a dual ROCK-AKT inhibitor in patients with solid tumors

Robert McLeod[1], Rajiv Kumar[2], Dionysis Papadatos-Pastos[2,], Joaquin Mateo[2], Jessica S Brown[2], Alvaro H Ingles Garces[2], Ruth Ruddle[3], Shaun Decordova[3], Simone Jueliger[4], Roberta Ferraldeschi[4], Oscar Maiques[5], Victoria Sanz-Moreno[5], Paul Jones[1], Stephanie Traub[1], Gavin Halbert[6], Sarah Mellor[1], Karen E Swales[3], Florence I Raynaud[3], Michelle D Garrett [3,7], Udai Banerji [2,3].

1. Cancer Research UK, London, UK
2. The Royal Marsden NHS Foundation Trust, London, UK
3. The Institute of Cancer Research, London, UK
4. Astex Pharmaceuticals, Cambridge, UK
5. Bart's Cancer Centre, Queen Mary University of London, London, UK
6. Strathclyde Institute of Pharmacy and Biomedical Sciences, Glasgow, UK
7. University of Kent, Canterbury, UK

Running title: Phase I trial of AT13148, a dual ROCK-AKT inhibitor

Key words: ROCK inhibitor; AKT inhibitor; poly-pharmacology; first-in-human; phase I

Corresponding Author:

Udai Banerji

NIHR Professor of Molecular Cancer Pharmacology

The Institute of Cancer Research and The Royal Marsden NHS Foundation Trust

Drug Development Unit, Sycamore House, Downs Road

Sutton, London, UK, SM2 5PT

Tel: +44 20 8661 3984

Email: udai.banerji@icr.ac.uk

Conflict of interest statement: AT13148 was discovered in a collaboration between The Institute of Cancer Research (ICR), Astex Therapeutics and Cancer Research UK (CRUK). RR, SD, KS, FR, MG and UB are (or were) employees of The ICR. RMcL, PJ, ST and SM are (or were) employees of CRUK. SJ and RF are (or were) employees of Astex Therapeutics. OS, VSM, RR, SD, KS, FR, MG and UB received funding from CRUK.

Word count: 3361, excluding abstract and refs; 2 tables; 4 figures; 1 supplementary figure; 1 supplementary table; 1 supplementary data file.

Translational relevance

AGC (protein family A, G and C) kinases are serine threonine kinases, which include ROCK, AKT and p70S6K. They are key anticancer targets with relevance to motility, metastasis, survival of cancer cells and an immune suppressive state within tumors. AT13148 is a potent ROCK and AKT inhibitor. The clinical tolerability profile was dominated by dose-limiting toxicities suggestive of ROCK inhibition (hypotension and headaches) and not AKT inhibition (hyperglycemia and rash). Careful consideration is warranted while developing multi-kinase inhibitors involving AGC kinases as they can have broad activity in preclinical models, but their clinical development using systemic routes of administration may be limited by side effect profiles related to potent inhibition of ROCK.

Abstract

Purpose

AT13148 is an oral AGC kinase inhibitor, which potently inhibits ROCK and AKT kinases. In preclinical models, AT13148 has been shown to have anti-metastatic and anti-proliferative activity.

Experimental Design

The trial followed a rolling six design during dose escalation. An intra-patient dose escalation arm to evaluate tolerability and a biopsy cohort to study pharmacodynamic (PD) effects were later added. AT13148 was administered orally three days a week (Mon-Wed-Fri) in 28-day cycles. Pharmacokinetic profiles were assessed using mass spectrometry and PD studies included quantifying p-GSK3β levels in platelet-rich plasma (PRP) and p-cofilin, p-MLC2 levels in tumor biopsies.

Results

Fifty-one patients were treated on study. The safety of 5 - 300 mg of AT13148 was studied. Further, the doses of 120-180-240 mg were studied in an intra-patient dose escalation cohort. The dose-limiting toxicities included hypotension (300 mg), pneumonitis and elevated liver enzymes (240 mg) and skin rash (180 mg). The most common side effects were fatigue, nausea, headaches and hypotension. Based on tolerability 180 mg was considered the maximally tolerated dose. At 180 mg, mean C_{max} and AUC were 383 nM and 13399 nM.h, respectively. At 180 mg, ≥50% reduction of p-cofilin was observed in 3/8 post-treatment biopsies.

Conclusions

AT13148 was the first dual potent ROCK-AKT inhibitor to be investigated for the treatment of solid tumors. The narrow therapeutic index and the pharmacokinetic profile led to recommend not developing this compound further. There are significant lessons learned in designing and testing agents that simultaneously inhibit multiple kinases including AGC kinases in cancer.

Introduction

Phosphoinositide 3-kinases (PI3Ks) are key mediators of intracellular signaling between the membrane-bound receptor tyrosine kinases (RTKs) and downstream effector molecules, such as AKT/PKB, m-TOR, GSK3β, S6K and S6, which control a range of vital cellular functions deregulated in cancer cells, including cellular growth, proliferation, and survival (1). There are currently multiple drugs licensed for use in the treatment of cancer in this pathway, ie PI3Kα, PI3Kδ and m-TOR inhibitors (2-5).

AGC kinases are a group of evolutionarily-related serine threonine kinases, some of which are deregulated in cancer (6). PDK1/PKA/PKB and S6K are key components of the PI3K pathway and have been targeted using a wide range of PI3K pathway inhibitors (1). However, there remain other AGC kinases such as Rho-associated coiled-coil containing protein kinase (ROCK) that influence growth (7-9) and metastasis of cancer cells independent of the PI3K pathway (10). ROCK-myosin II signaling has also recently been shown to be important in modulating resistance to targeted therapy in melanoma and an immunosuppressive environment within tumors (11).

AT13148 was discovered using a high throughput x-ray crystallography and fragment-based drug design as an AGC kinase inhibitor that inhibited AKT and other AGC kinases such as ROCK (12). It was hypothesized that additional AGC kinase activity would result in increased anti-proliferative and anti-metastatic efficacy and possibly reduce resistance to selective AKT inhibition (13,14). Preclinical studies have evaluated the efficacy of AT13148 in blocking invasion and metastasis in melanoma and pancreatic cancer models (14,15). In addition, AT13148 has been shown to inhibit PI3K signaling and induce cell death in a range of preclinical models, including gastric and prostate cancer models (13,16). There are currently multiple selective AKT inhibitors in late stages of clinical

development (17) and ROCK inhibitors are licensed for use in non-oncological indications, such as pulmonary hypertension (18), but have not been clinically tested in cancer patients until now. Herein, we report the results from the first-in-human phase I study of AT13148, a potent dual AKT/ROCK inhibitor, in adults with advanced solid tumors.

Material and Methods

Design

The study followed a rolling 6 dose escalation design (19). Following an amendment, two cohorts were added. The first included an intra-patient dose escalation in patients at dose levels 120-180-240 mg starting with one week dosing at the lowest dose followed by escalating to the next dose of 180 mg until the highest dose of 240 mg during cycle 1. The aim of this cohort was to evaluate if the on-target hypotension would be better tolerated if the dose was increased in a stepwise fashion. The second amendment introduced a mandatory biopsy cohort where fresh biopsies were collected before and after treatment at the recommended phase II dose (RP2D) of 180 mg. The trial was conducted to ethical principles laid down by the Declaration of Helsinki and the protocol was reviewed by regulatory agencies (MHRA, UK) and a UK national research ethics committee. Written informed consent was obtained (patients were given an information sheet and signed a consent form) prior to patients enrolling in the clinical trial. Inclusion criteria included the fact that patients had received standard-of-care treatment for their metastatic solid tumors and had adequate renal and hepatic function (full inclusion and exclusion criteria in Supplementary Data). Key exclusion criteria included an abnormal fasting blood sugar and a history of hypertension on anti-hypertensive medication.

AT13148 was administered orally three days a week (Mon-Wed-Fri) in 28-day cycles. Patients were seen weekly for toxicity assessments and imaging to evaluate tumor response was conducted every 2 cycles.

Pharmacokinetics

A single dose of AT13148 was administered 7 days before cycle 1 for pharmacokinetic analysis. A full pharmacokinetic profile was also carried out on cycle 2, day 1. Blood was collected at baseline, 15 minutes, 30 minutes, 1, 2, 6, 12, 24, 48, 72 and 96 hours post-dose for analysis (the last two being optional from Cohort 6, 160 mg, cycle 1). Plasma concentrations of AT1318 were measured by liquid chromatography mass spectrometry (see Supplementary Data) Pharmacokinetic parameters were derived from Phoenix WinNonlin using non-compartmental analysis.

Pharmacodynamics

Blood samples for pharmacodynamics were taken at baseline, 2 hrs, 6 hrs, 24 hrs and 48 hrs after treatment on the run-in dose at day -47 to -4 and on cycle 2, day 1. Phosphorylation of GSK3β Ser9 (p-GSK3β) was quantified in platelet-rich plasma (PRP) extracted from serial blood samples using electrochemiluminescent immunoassays on the MesoScale Discovery (MSD®) technology platform using previously validated techniques (20). Relative changes in p-GSK3β were reported as a ratio, calculated as the percentage of baseline levels normalized to total GSK3β. Phosphorylated cofilin protein levels in tumor biopsies pre-dose and post-AT13148 treatment (between cycle 1, day 15 or cycle 2, day 1, 24 hrs post-treatment) were measured using the Protein Simple WES Assay platform. Changes in phospho- and total cofilin normalized to GAPDH were measured in the form of chemiluminescence signals with the area under the curve (AUC)

calculated for each analyte by the WES Compass software. Relative changes in phosphorylated cofilin were reported as a percentage of pre-dose protein levels.

Phosphorylation of MLC2 was quantified using immunohistochemistry (IHC). Four-µm thick sections were incubated at 60° C for 20 min and then subjected to antigen retrieval using Access Super Tris pH 9 buffer (A Menarini Diagnostics) at 110° C for 6 min in a Decloaking Chamber NxGen (Biocare Medical). Samples were blocked with Dual Endogenous Enzyme-Blocking Reagent (Dako) for 10 min and were then incubated with primary antibodies for 40 min at room temperature (RT), washed and then incubated with biotinylated secondary antibodies (rabbit, mouse or rat; 1:200; Vector-Labs) for 30 min at RT. Signal was then amplified using a VECTASTAIN ABC HRP kit (PK-4000) for 20 min at RT and the reaction was developed using VIP substrate (SK-4600, Vector-Labs) for 10 min at RT. Stainings were counterstained with hematoxylin. The slides were imaged using a NanoZoomer S210 slide scanner (Hamamatsu, Japan). Staining quantification was performed using QuPath 0.1.2. In order to quantify p-MLC2, the images were analyzed using positive cell detection and three different thresholds were applied according to the intensity scores (0, 1, 2 and 3). Next, the software was trained by creating a random trees classification algorithm combined with the intensity information in order to differentiate tumor from stroma, necrosis and immune cells (21).

Results

Patient characteristics

A total of 56 patients with solid tumors who had previously received standard-of-care treatment were enrolled on the study from December 2012 to December 2017, of whom 51 patients received at least one dose of AT13148. The demographics of the patients

included a male/female ratio of 25/31, age range of 34 - 76 yrs and the most common tumor types were colorectal and breast cancer **(Supplementary Table 1).**

Safety

Patients were initially treated across a dose rage of 5 – 300 mg a day in 8 cohorts following a rolling six design during the dose escalation. Two further cohorts were then added: first, a cohort that included intra-patient dose escalation (Cohort 9) over 3 dose levels (120 mg -180 mg - 240 mg) to evaluate whether incremental increase of dose over a period of 3 weeks could improve tolerability; then, a mandatory biopsy cohort of patients was treated at the RP2D of 180 mg (Cohort 10) to study pharmacodynamic effects in pre- and post-treatment biopsies **(Figure 1)**.

The dose escalation proceeded by dose doubling from 5 - 160 mg with no dose-limiting toxicities reported. At the dose of 160 mg (Cohort 6), following multiple non-dose-limiting toxicity (DLT) grade 3 toxicities of hypotension and diarrhea, the dose escalation proceeded by a 50% increase to 240 mg (Cohort 7). There was one DLT of elevated liver enzymes seen at 240 mg in addition to multiple episodes of grade 2 toxicities such as nausea, fatigue, anorexia and hypotension. As only 1 in 6 evaluable patients had a DLT, the dose was escalated cautiously by a further 25% to 300 mg (Cohort 8). At this dose level, two patients experienced grade 2 hypotension, one patient experienced grade 3 hypotension and one patient experienced grade 4 hypotension with a systolic blood pressure of less than 40 mm Hg requiring inotropic support. No further patients were treated at the dose of 300 mg following the adverse event. In Cohort 9 (intra-patient dose escalation cohort), two DLTs (grade 3 pneumonitis at 240 mg and grade 3 rash at 180 mg) were reported. However, multiple grade 1 and 2 toxicities including grade 2 fatigue were seen at 240 mg and limited continuation of this approach. The dose was therefore de-

escalated and the maximally tolerated dose was established at a dose of 180 mg AT13148 orally given on days 1, 3 and 5 of each week. As a composite of the flat dose escalation and the intra-patient dose escalation cohort, a dose of 180 mg was considered the maximally tolerated dose of AT13148.

The most common treatment related side effects were hypotension, nausea, headache and fatigue **(Table 1).** There were four grade 3 or 4 events that were considered dose-limiting toxicities, which included hypotension at 300 mg, elevated transaminases and pneumonitis at 240 mg and a maculopapular rash at 180 mg.

The most common known on-target toxicity of AT13148 included hypotension. This was often associated with headaches and occurred within 8 hrs of dosing. Fatigue and nausea were commonly seen at or above the dose level 160 mg. Although one episode of elevated liver enzymes was described as a dose-limiting toxicity in Cohort 7 (240 mg), there were no dose-dependent trends of increased liver transaminases across different dose levels. Rash was seen in 6/51 (11.8%) of patients but was dose-limiting in only one patient.

Pharmacokinetics

AT13148 was measured in plasma in all patients and data was obtained from 44 patients across nine cohorts (flat dose Cohorts 1 - 8 and 10). Data was limited from Cohort 8 (300 mg AT13148) as there were only three evaluable patients, and only one patient received a second cycle of AT13148.

Maximum plasma concentrations in cycle 1 ranged between 7 and 964 nmol/L with mean values of 22 to 661 nmol/L. In cycle 2, plasma concentrations of AT13148 were between 18 and 1097 nmo/L with mean values of 24 to 712 nmol/L. There was a dose-related

increase in the mean C_{max} and AUC r^2 = 0.97 and 0.98, respectively **(Supplementary Figure 1)**, however, a high intra-patient variability was observed at doses of 80 mg and above. In many instances (34 patient profiles of the 55), the terminal $t_{½}$ was not accurately established, which also affected related PK parameters (clearance, volume of distribution etc.). This was addressed with additional (optional) sampling times over 48 hours (at 72 and 96 hours). Based on 14 evaluable patients in cycle 1, the half-life of AT13148 ranged between 14.4 and 32.2 hours **(Table 2)**. At the tolerable dose of 180 mg free drug levels or exposure were below those measured in preclinical efficacy experiments.

PK-hypotension relationships

Due to the ROCK inhibitory activity of the drug, hypotension was regarded as both an on-target toxicity (22) and a pharmacodynamic biomarker. The maximum decrease in supine systolic blood pressure and C_{max} or AUC_{last} were studied. Where there was matched data for blood pressure and plasma drug concentrations available, there was a weak linear correlation seen between hypotension and both C_{max} and $AUC_{0\text{-}last}$ (r^2 0.25 and 0.17, respectively) **(Figure 2)**. However, looking at individual cases, of the eight patients with the most severe hypotension (a fall of greater than 30 mm Hg) six patients had high exposure in terms of C_{max} >350 nM and $AUC_{0\text{-}last}$ >1000 nM·h. The high incidence of hypotension found at high doses became dose-limiting to the trial and halted recruitment at 300 mg.

Pharmacodynamics

Phosphorylation of GSK3β was quantified in platelet-rich plasma to assess AKT inhibition. At doses 160-300 mg there was a weak trend in the relationship between the plasma concentration and the p-GSK3β levels; r^2 =0.17 **(Figure 3A).** At the non-tolerated dose

level of 300 mg, there was a statistically significant reduction of p-GSK3β levels in platelet-rich plasma 2 - 6 hrs after treatment when compared to predose **(Figure 3B)**. We also studied the phosphorylation of cofilin, a known downstream effector of ROCK activity in pre- and post-treatment biopsies at the 180 mg dose level. Of the 8 pre- and post-treatment biopsies conducted, 5/8 showed a reduction of p-cofilin in post-treatment biopsies and 3/8 showed >50% reduction of p-cofilin **(Figure 4A).** Myosin II is regulated by ROCK via direct phosphorylation of the regulatory light chain (MLC2). p-MLC2 was assayed using immunohistochemistry in 5 paired biopsies and there was a reduction in H scores in post- treatment samples in 1/5 paired biopsies **(Figure 4B).**

Clinical efficacy

No complete or partial responses were seen in the study. The median number of cycles of AT13148 on the study was 2 (range 1 - 10). One patient with NSCLC (adenocarcinoma) was on the study for 10 cycles and had been tested and shown not to have an EGFR mutation or ALK rearrangement as part of their standard-of-care.

Discussion

AT13148 is an AGC kinase inhibitor with potent ROCK and AKT inhibitory activity (13). ROCK inhibitors have attracted interest due to their role in tumor invasion, cancer metastasis and stromal remodelling (23,24). In addition, there are a number of studies demonstrating preclinical anti-proliferative activity in melanoma (7), neuroblastoma (9), pancreatic cancer (15), lung cancer and leukemia (8). AT13148, to our knowledge, is the first dual ROCK-AKT inhibitor that has been evaluated in a clinical trial as an anticancer agent.

Vasodilation caused by ROCK inhibition led to a high number of patients who received AT13148 experiencing hypotension, which was dose-limiting at a dose of 300 mg. Though not dose-limiting, headaches were a common toxicity seen in this study and were also likely to be due to vasodilatation. This property of ROCK inhibitors has led to its use in pulmonary hypertension (25) and in the treatment of cerebral vasospasm following subarachnoid hemorrhage (26). Other dose-limiting toxicities included pneumonitis and skin rash; these have previously been reported in agents such as PI3K, AKT or m-TOR inhibition (2,5,20,27-29). One dose-limiting toxicity of elevated liver enzymes was seen. Elevated liver enzymes have been reported in PI3K pathway inhibitors but it is not clear if this an on-target toxicity (30,31). Nausea and fatigue were other common toxicities, which were non-specific and have been reported across a wide range of other anticancer drugs. Interestingly, hyperglycemia and non-neutropenic infections, which are common features of PI3K pathway inhibitors, were not commonly seen in this study (32,33).

The pharmacokinetic profile of AT13148 showed a high degree of variability when administered in the current formulation. This led to considerable overlap between exposure to AT13148 at dose levels of 160 mg and above. This was considered a challenge and risk for further development of the current formulation of the drug considering the narrow therapeutic index.

Interestingly, postural hypotension was seen at dose levels above 80 mg, suggestive of ROCK inhibition. Therefore, we decided to study the relationship of Cmax and AUC of AT13148 to changes in blood pressure where matched data points were available. This showed a low to moderate correlation. Pharmacodynamic analysis in platelet-rich plasma demonstrated a transient reduction of p-GSK3β levels at the non-tolerable dose of 300 mg; a trend towards reduction of levels of p-GSK3β between 160 - 300 mg. Reduction of p-

GSK3β has been shown to be a reproducible biomarker of AKT inhibition (20,34) and reduction of p-GSKRβ was demonstrated in xenograft models treated with AT13148 showing growth delay (13). Finally, there was a 50% reduction in phosphorylation of cofilin in 3/8 patients and reduction in the phosphorylation of MLC2 in only 1/5 paired biopsies studied with pre- and post-tumor biopsies at the dose level of 180 mg. A reduction of p-MLC2 has been shown to be a biomarker of ROCK inhibition in AT13148-treated mice in-vivo. However, measurement of p-MLC2 levels in xenograft tissue that had shown tumor growth delay has not been performed (14,15), thus, even if a reduction of p-MLC2 was demonstrable in all samples, interpretation of the data would need to be put into this context. The phosphorylation of coflin has been shown to be a biomarker of ROCK inhibition (7), but specific experiments measuring p-cofilin in xenografts of AT13148-treated mice have not been performed and thus it is difficult to interpret the findings in this study. However, given that changes in both the biomarkers were not seen in a majority of the samples treated at the RP2D of 180 mg thrice a week, these findings were not suggestive of consistent and robust ROCK inhibition in tumor tissue.

There were no clinical responses seen in the study. The reasons for lack of single agent response could be many. The anticancer activity of ROCK inhibitors is predominantly towards causing a reduction in metastatic spread. This first-in-human study was geared towards defining tolerability and PK-PD relationships, and recruited patients with advanced solid tumors. It would not be possible to study anti-metastatic activity of such a drug in these patients: the dose-limiting on-target toxicity of hypotension limited the escalation to biological effective levels of ROCK inhibition in tumor tissue. Further, the hypotension limited the ability to sufficiently inhibit other key AGC kinases such as AKT, which contributed to anti-proliferative activity in preclinical models. Prospective sequencing of tumor to enrich cohorts with patients whose tumors had *PIK3CA* or *AKT* mutations would

have improved the chances of observing responses but, given that there were no toxicities or consistent biomarker changes suggestive of AKT inhibition, this would have been unlikely. Future research into ROCK inhibitors could consider isoform specific ROCK II inhibitors that may cause reduced hypotension and the possibility of topical applications for selected skin cancers, which could reduce other systemic side effects (18).

The pharmacological audit trail defines multiple factors involved in go-no-go decisions in drug development (35). The current first-in-human study demonstrated multiple factors that would make further development of this agent challenging, including its toxicity seen, variable pharmacokinetic profile and inability to reproducibly inhibit AGC kinases in tumor tissue.

AT13148 also brings poly-pharmacology of anticancer drugs into question. It is increasingly found that targeted anticancer drugs inhibit multiple targets (36,37). Importantly, this has led to drugs which inhibit multiple targets being licensed for indications which are relevant to one target and not to the other e.g. sorafenib is licensed in renal cancer for its VEGFR inhibitory activity and not in melanoma for its RAF inhibitory activity (38,39) and crezotinib has been licensed in lung cancer for its ALK inhibitory activity and not as an MET inhibitor (40,41). AT13148 inhibited multiple AGC kinases and was found to cause cell death and apoptosis when compared to more selective AKT inhibitors in-vitro. In a biochemical screen, AT13148 was a more potent ROCK inhibitor compared to an AKT inhibitor. The IC_{50} of AT13148 for ROCK I and ROCK 2 was 6 nM and 4 nM, respectively, when compared to that for AKT1, AKT2 and AKT3, 38 nM, 402 nM and 50 nM, respectively (13). The additional putative cytotoxic anticancer effects of ROCK I/II inhibitory activity of AT13148 could not be exploited due to clinical hypotension caused by its activity on normal tissue. The current trial raises a further important issue

surrounding cancer drugs that can, by virtue of inhibiting multiple kinases, target the cardiovascular system (eg VEGFR or vascular disrupting agents). In these instances, it could be hypothesized that cells of the vasculature are likely to be exposed to the drug earlier than cells of tumors and possibly at a higher concentration, resulting in cardiovascular adverse events being limiting: for example, the multikinase inhibitor, ilorasertib, targeted the VEGFR and Aurora kinase families resulting in the VEGR-related adverse events being limiting (42). In the case of AT13148 it is difficult to know if the cardiovascular side effects occurred at lower concentrations required for AKT inhibition because the drug inhibits ROCK more potently or because cells in the vascular system are likely to be exposed to such drugs earlier, and to a possibly higher concentration, than cancer cells in the tumor.

This clinical information will be of importance to researchers developing ROCK inhibitors or other AGC kinases as anticancer drugs and makes the case for the development of specific inhibitors of individual AGC kinases.

Acknowledgements

AT13148 was discovered in a collaboration between The Institute of Cancer Research and Astex Pharmaceuticals, UK. U Banerji and MD Garrett acknowledge funding for the clinical trial from Cancer Research UK (CRUK) (Ref: 9098). R Kumar, D Papadatos-Pastos, J Mateo, JS Brown, AH Ingles Garces, R Ruddle, S Decordova, KE Swales, MD Garrett, FI Raynaud and U Banerji acknowledge institutional funding from CRUK as part of the Experimental Cancer Medicine Centre initiative (Ref: C12540/ A25128); R Ruddle, MD Garrett, FI Raynaud and U Banerji acknowledge a CRUK Cancer Therapeutics Unit award to the Institute of Cancer Research (Ref: C2739/A22897); KE Swales, MD Garrett, FI Raynaud and U Banerji acknowledge a CRUK Cancer Therapeutics Centre award (Ref:

C309/A25144). R Kumar, D Papadatos-Pastos, J Mateo, JS Brown, AH Ingles Garces, R Ruddle, S Decordova, KE Swales, MD Garrett, FI Raynaud and U Banerji also acknowledge the National Institute for Health Research (NIHR) Biomedical Research Centre initiative awarded to The Institute of Cancer Research and The Royal Marsden NHS Foundation Trust (Ref: IS-BRC-1215-20021). V Sanz-Moreno and O Maiques acknowledge a CRUK award (Ref: C33043/A24478) for the laboratory work, and funding from Bart's Charity. U Banerji is a recipient of an NIHR Research Professorship award (Ref: RP2016-07-028).

References

1. Janku F, Yap TA, Meric-Bernstam F. Targeting the PI3K pathway in cancer: are we making headway? Nat Rev Clin Oncol **2018**;15(5):273-91 doi 10.1038/nrclinonc.2018.28.
2. Andre F, Ciruelos E, Rubovszky G, Campone M, Loibl S, Rugo HS*, et al.* Alpelisib for PIK3CA-Mutated, Hormone Receptor-Positive Advanced Breast Cancer. N Engl J Med **2019**;380(20):1929-40 doi 10.1056/NEJMoa1813904.
3. Furman RR, Sharman JP, Coutre SE, Cheson BD, Pagel JM, Hillmen P*, et al.* Idelalisib and rituximab in relapsed chronic lymphocytic leukemia. N Engl J Med **2014**;370(11):997-1007 doi 10.1056/NEJMoa1315226.
4. Dreyling M, Morschhauser F, Bouabdallah K, Bron D, Cunningham D, Assouline SE*, et al.* Phase II study of copanlisib, a PI3K inhibitor, in relapsed or refractory, indolent or aggressive lymphoma. Ann Oncol **2017**;28(9):2169-78 doi 10.1093/annonc/mdx289.
5. Baselga J, Campone M, Piccart M, Burris HA, 3rd, Rugo HS, Sahmoud T*, et al.* Everolimus in postmenopausal hormone-receptor-positive advanced breast cancer. N Engl J Med **2012**;366(6):520-9 doi 10.1056/NEJMoa1109653.

6. Leroux AE, Schulze JO, Biondi RM. AGC kinases, mechanisms of regulation and innovative drug development. Semin Cancer Biol **2018**;48:1-17 doi 10.1016/j.semcancer.2017.05.011.

7. Kumper S, Mardakheh FK, McCarthy A, Yeo M, Stamp GW, Paul A*, et al.* Rho-associated kinase (ROCK) function is essential for cell cycle progression, senescence and tumorigenesis. Elife **2016**;5:e12994 doi 10.7554/eLife.12203.

8. Mali RS, Ramdas B, Ma P, Shi J, Munugalavadla V, Sims E*, et al.* Rho kinase regulates the survival and transformation of cells bearing oncogenic forms of KIT, FLT3, and BCR-ABL. Cancer Cell **2011**;20(3):357-69 doi 10.1016/j.ccr.2011.07.016.

9. Dyberg C, Fransson S, Andonova T, Sveinbjornsson B, Lannerholm-Palm J, Olsen TK*, et al.* Rho-associated kinase is a therapeutic target in neuroblastoma. Proc Natl Acad Sci U S A **2017**;114(32):E6603-E12 doi 10.1073/pnas.1706011114.

10. Narumiya S, Thumkeo D. Rho signaling research: history, current status and future directions. FEBS Lett **2018**;592(11):1763-76 doi 10.1002/1873-3468.13087.

11. Orgaz JL, Crosas-Molist E, Sadok A, Perdrix-Rosell A, Maiques O, Rodriguez-Hernandez I*, et al.* Myosin II Reactivation and Cytoskeletal Remodeling as a Hallmark and a Vulnerability in Melanoma Therapy Resistance. Cancer Cell **2020**;37(1):85-103 e9 doi 10.1016/j.ccell.2019.12.003.

12. Saxty G, Woodhead SJ, Berdini V, Davies TG, Verdonk ML, Wyatt PG*, et al.* Identification of inhibitors of protein kinase B using fragment-based lead discovery. J Med Chem **2007**;50(10):2293-6 doi 10.1021/jm070091b.

13. Yap TA, Walton MI, Grimshaw KM, Te Poele RH, Eve PD, Valenti MR*, et al.* AT13148 is a novel, oral multi-AGC kinase inhibitor with potent pharmacodynamic and antitumor activity. Clin Cancer Res **2012**;18(14):3912-23 doi 10.1158/1078-0432.CCR-11-3313.

14. Sadok A, McCarthy A, Caldwell J, Collins I, Garrett MD, Yeo M*, et al.* Rho kinase inhibitors block melanoma cell migration and inhibit metastasis. Cancer Res **2015**;75(11):2272-84 doi 10.1158/0008-5472.CAN-14-2156.

15. Rath N, Munro J, Cutiongco MF, Jagiello A, Gadegaard N, McGarry L*, et al.* Rho Kinase Inhibition by AT13148 Blocks Pancreatic Ductal Adenocarcinoma Invasion and Tumor Growth. Cancer Res **2018**;78(12):3321-36 doi 10.1158/0008-5472.CAN-17-1339.

16. Xi Y, Niu J, Shen Y, Li D, Peng X, Wu X. AT13148, a first-in-class multi-AGC kinase inhibitor, potently inhibits gastric cancer cells both in vitro and in vivo. Biochem Biophys Res Commun **2016**;478(1):330-6 doi 10.1016/j.bbrc.2016.01.167.

17. Brown JS, Banerji U. Maximising the potential of AKT inhibitors as anti-cancer treatments. Pharmacol Ther **2017**;172:101-15 doi 10.1016/j.pharmthera.2016.12.001.

18. Feng Y, LoGrasso PV, Defert O, Li R. Rho Kinase (ROCK) Inhibitors and Their Therapeutic Potential. J Med Chem **2016**;59(6):2269-300 doi 10.1021/acs.jmedchem.5b00683.

19. Skolnik JM, Barrett JS, Jayaraman B, Patel D, Adamson PC. Shortening the timeline of pediatric phase I trials: the rolling six design. J Clin Oncol **2008**;26(2):190-5 doi 10.1200/JCO.2007.12.7712.

20. Banerji U, Dean EJ, Perez-Fidalgo JA, Batist G, Bedard PL, You B*, et al.* A Phase I Open-Label Study to Identify a Dosing Regimen of the Pan-AKT Inhibitor AZD5363 for Evaluation in Solid Tumors and in PIK3CA-Mutated Breast and Gynecologic Cancers. Clin Cancer Res **2018**;24(9):2050-9 doi 10.1158/1078-0432.CCR-17-2260.

21. Bankhead P, Loughrey MB, Fernandez JA, Dombrowski Y, McArt DG, Dunne PD*, et al.* QuPath: Open source software for digital pathology image analysis. Sci Rep **2017**;7(1):16878 doi 10.1038/s41598-017-17204-5.

22. Kikuchi Y, Takahashi J, Hao K, Sato K, Sugisawa J, Tsuchiya S*, et al.* Usefulness of intracoronary administration of fasudil, a selective Rho-kinase inhibitor, for PCI-related refractory myocardial ischemia. Int J Cardiol **2019**;297:8-13 doi 10.1016/j.ijcard.2019.09.057.

23. Georgouli M, Herraiz C, Crosas-Molist E, Fanshawe B, Maiques O, Perdrix A*, et al.* Regional Activation of Myosin II in Cancer Cells Drives Tumor Progression via a Secretory Cross-Talk with the Immune Microenvironment. Cell **2019**;176(4):757-74 e23 doi 10.1016/j.cell.2018.12.038.

24. Herraiz C, Calvo F, Pandya P, Cantelli G, Rodriguez-Hernandez I, Orgaz JL*, et al.* Reactivation of p53 by a Cytoskeletal Sensor to Control the Balance Between DNA Damage and Tumor Dissemination. J Natl Cancer Inst **2016**;108(1) doi 10.1093/jnci/djv289.

25. Fukumoto Y, Yamada N, Matsubara H, Mizoguchi M, Uchino K, Yao A*, et al.* Double-blind, placebo-controlled clinical trial with a rho-kinase inhibitor in pulmonary arterial hypertension. Circ J **2013**;77(10):2619-25 doi 10.1253/circj.cj-13-0443.

26. Tanaka K, Minami H, Kota M, Kuwamura K, Kohmura E. Treatment of cerebral vasospasm with intra-arterial fasudil hydrochloride. Neurosurgery **2005**;56(2):214-23; discussion -23 doi 10.1227/01.neu.0000147975.24556.bc.

27. Sarker D, Ang JE, Baird R, Kristeleit R, Shah K, Moreno V*, et al.* First-in-human phase I study of pictilisib (GDC-0941), a potent pan-class I phosphatidylinositol-3-kinase (PI3K) inhibitor, in patients with advanced solid tumors. Clin Cancer Res **2015**;21(1):77-86 doi 10.1158/1078-0432.CCR-14-0947.

28. Saura C, Roda D, Rosello S, Oliveira M, Macarulla T, Perez-Fidalgo JA*, et al.* A First-in-Human Phase I Study of the ATP-Competitive AKT Inhibitor Ipatasertib Demonstrates Robust and Safe Targeting of AKT in Patients with Solid Tumors. Cancer Discov **2017**;7(1):102-13 doi 10.1158/2159-8290.CD-16-0512.

29. Basu B, Dean E, Puglisi M, Greystoke A, Ong M, Burke W*, et al.* First-in-Human Pharmacokinetic and Pharmacodynamic Study of the Dual m-TORC 1/2 Inhibitor AZD2014. Clin Cancer Res **2015**;21(15):3412-9 doi 10.1158/1078-0432.CCR-14-2422.

30. Blagden S, Omlin A, Josephs D, Stavraka C, Zivi A, Pinato DJ*, et al.* First-in-human study of CH5132799, an oral class I PI3K inhibitor, studying toxicity, pharmacokinetics, and pharmacodynamics, in patients with metastatic cancer. Clin Cancer Res **2014**;20(23):5908-17 doi 10.1158/1078-0432.CCR-14-1315.

31. Naing A, Aghajanian C, Raymond E, Olmos D, Schwartz G, Oelmann E*, et al.* Safety, tolerability, pharmacokinetics and pharmacodynamics of AZD8055 in advanced solid tumours and lymphoma. Br J Cancer **2012**;107(7):1093-9 doi 10.1038/bjc.2012.368.

32. Geuna E, Roda D, Rafii S, Jimenez B, Capelan M, Rihawi K*, et al.* Complications of hyperglycaemia with PI3K-AKT-mTOR inhibitors in patients with advanced solid tumours on Phase I clinical trials. Br J Cancer **2015**;113(11):1541-7 doi 10.1038/bjc.2015.373.

33. Rafii S, Roda D, Geuna E, Jimenez B, Rihawi K, Capelan M*, et al.* Higher Risk of Infections with PI3K-AKT-mTOR Pathway Inhibitors in Patients with Advanced Solid Tumors on Phase I Clinical Trials. Clin Cancer Res **2015**;21(8):1869-76 doi 10.1158/1078-0432.CCR-14-2424.

34. Yap TA, Yan L, Patnaik A, Tunariu N, Biondo A, Fearen I*, et al.* Interrogating two schedules of the AKT inhibitor MK-2206 in patients with advanced solid tumors

incorporating novel pharmacodynamic and functional imaging biomarkers. Clin Cancer Res **2014**;20(22):5672-85 doi 10.1158/1078-0432.CCR-14-0868.

35. Banerji U, Workman P. Critical parameters in targeted drug development: the pharmacological audit trail. Semin Oncol **2016**;43(4):436-45 doi 10.1053/j.seminoncol.2016.06.001.

36. Antolin AA, Workman P, Mestres J, Al-Lazikani B. Polypharmacology in Precision Oncology: Current Applications and Future Prospects. Curr Pharm Des **2016**;22(46):6935-45 doi 10.2174/1381612822666160923115828.

37. Antolin AA, Ameratunga M, Banerji U, Clarke PA, Workman P, Al-Lazikani B. The kinase polypharmacology landscape of clinical PARP inhibitors. Sci Rep **2020**;Eupub.

38. Escudier B, Eisen T, Stadler WM, Szczylik C, Oudard S, Siebels M*, et al.* Sorafenib in advanced clear-cell renal-cell carcinoma. N Engl J Med **2007**;356(2):125-34 doi 10.1056/NEJMoa060655.

39. Eisen T, Ahmad T, Flaherty KT, Gore M, Kaye S, Marais R*, et al.* Sorafenib in advanced melanoma: a Phase II randomised discontinuation trial analysis. Br J Cancer **2006**;95(5):581-6 doi 10.1038/sj.bjc.6603291.

40. Solomon BJ, Mok T, Kim DW, Wu YL, Nakagawa K, Mekhail T*, et al.* First-line crizotinib versus chemotherapy in ALK-positive lung cancer. N Engl J Med **2014**;371(23):2167-77 doi 10.1056/NEJMoa1408440.

41. Landi L, Chiari R, Tiseo M, D'Inca F, Dazzi C, Chella A*, et al.* Crizotinib in MET deregulated or ROS1 rearranged pretreated non-small-cell lung cancer (METROS): a phase II, prospective, multicentre, two-arms trial. Clin Cancer Res **2019** doi 10.1158/1078-0432.CCR-19-0994.

42. Maitland ML, Piha-Paul S, Falchook G, Kurzrock R, Nguyen L, Janisch L*, et al.* Clinical pharmacodynamic/exposure characterisation of the multikinase inhibitor

ilorasertib (ABT-348) in a phase 1 dose-escalation trial. Br J Cancer **2018**;118(8):1042-50 doi 10.1038/s41416-018-0020-2.

Treatment Emergent Adverse Event	Total No. subjects (n = 51)	Cohort 1 5 mg (n=4)			Cohort 2 10 mg (n=5)			Cohort 3 20 mg (n=3)			Cohort 4 40 mg (n=3)			Cohort 5 80 mg (n=4)			Cohort 6 160 mg (n=7)			Cohort 7 240 mg (n=6)			Cohort 8 300 mg (n=5)				Cohort 9 120-180-240 mg (n=7)			Cohort 10 180 mg (n=7)		
		1	2	3	1	2	3	1	2	3	1	2	3	1	2	3	1	2	3	1	2	3	1	2	3	4	1	2	3	1	2	3
GASTROINTESTINAL DISORDERS																																
Diarrhea	7 (13.7%)																		1	1							2			3		
Nausea	15 (29.4%)	1															3			1	1		2				4			3		
Vomiting	7 (13.7%)																1			3			1				1			1		
GENERAL DISORDERS AND ADMINISTRATION SITE CONDITIONS																																
Fatigue	9 (17.6%)		1																	1	1						2	2		2		
METABOLISM AND NUTRITION DISORDERS																																
Anorexia	7 (13.7%)	1																1			2						2			1		
NERVOUS SYSTEM DISORDERS																																
Headache	12 (23.5%)																1	2		2			3							4		
VASCULAR DISORDERS																																
Flushing	6 (11.8%)																	1		2	1		1							1		
Hypotension	20 (39.2%)				1												3	1	1	3	1			3	1	1	2			1		2

Table 1.

Treatment emergent adverse events

Cycle 1		Tmax (h)	Cmax (nmol/L)	HL Lambda z (h)	AUClast (h*nmol/L)	* AUC to 48 h (h*nmol/L)	AUCINF obs (h*nmol/L)	Vz F obs (L)	Cl F obs (L/h)
Cohort 1 5mg	Mean	5	20	60	400	400	900	1400	20
	SD	5	15	27	21	210	350	290	11
	% CV	97	70.0	41	54	54	40	21	60
Cohort 2 10mg	Mean	6	15	40	300	300	600	1900	100
	SD	4.2	4.8	30	190	190	460	670	95
	% CV	75	32	85.0	66	66	77	36	96
Cohort 3 20mg	Mean	4	30	20	600	600	1000	2000	90
	SD	2.8	16	13	440	440	750	660	72
	% CV	66	46	56	70	70	78	32	83
Cohort 4 40mg	Mean	1.99	120	15	1900	1900	2100	1100	50
	SD	0.03	21	1.00	540	540	630	310	17
	% CV	2	18	7	29	29	30	28	33
Cohort 5 80mg	Mean	3	180	50	5000	5000	10000	1600	30
	SD	2	69	44	3000	3000	16000	910	22
	% CV	67	38	82	61	61	118	57	67
Cohort 6 160mg	Mean	5	400	40	12000	10000	20000	2000	40
	SD	2	290	22	7900	5900	16000	1300	28
	% CV	41	66	52	64	57	79	72	75
Cohort 7 240mg	Mean	5	500	40	15000	13000	30000	2000	50
	SD	2	280	17	9000	9000	24000	930	36
	% CV	40.0	61	44	63	70	94	48	80
Cohort 8 300mg	Mean	6.1	700	60	20000	20000	40000	1400	18
	SD	0.12	130	35	4100	4100	10000	600	4.8
	% CV	2	20	57	21	21	23	42	26
Cohort 10 180mg	Mean	4	400	40	13000	9000	20000	2000	50
	SD	2.3	190	21	8000	4700	14000	2200	59
	% CV	64	50	51	60	52	74	94	110

Table 2.

Pharmacokinetic parameters of AT13148

The pharmacokinetic parameters between 5 - 300 mg in cycle 1. There was considerable variation of AUC and Cmax at doses of 160 mg and above.

LEGENDS TO FIGURES

Figure 1

The dose escalation scheme

Dose was doubled from 5 - 160 mg, following which a more conservative increase in dose to 240 mg and 300 mg was evaluated. Following grade 4 hypotension being seen at 300 mg an intra-patient dose escalation schedule was explored to evaluate if this improved tolerability of higher doses. The dose of 180 mg was considered tolerated pre- and post- treatment biopsies were conducted to evaluate pharmacodynamics effects.

Figure 2

Relationship of hypotension and pharmacokinetic parameters

The maximum drop in supine systolic blood pressure was measured and correlated with PK profiles of individual patients in patients where matched blood pressure and PK measurements were available at doses 160 mg, 240 mg and 300 mg. A) Relationship between AUC and drop in blood pressure $r^2 = 0.17$. B) Relationship between Cmax and maximal drop in blood pressure $r^2 = 0.25$.

Figure 3

Pharmacodynamic effects in platelet-rich plasma

Phosphorylation of GSK3β is a downstream event of AKT activation and reduction of p-GSK3β was quantified in platelet rich plasma before and after treatment with AT13148. A) The relationship of the plasma levels of AT13148 and p-GSK3β across the dose levels

of 160 - 300 mg. There was a trend towards reduction of p-GSK3β and increasing plasma levels of AT13148, $r^2 = 0.17$, $p = 0.0354$. B) p-GSK3β normalized to total GSK3β levels were reduced between 2 - 24 hrs after treatment of AT3148 at the 300 mg cohort. The asterisk indicates significance in Dunnett's test. The changes were not significant at doses lower than 300 mg.

Figure 4

Pharmacodynamic effects in tumor tissue

Biopsies were done at the dose level of 180 mg thrice a week. Phosphorylation of cofilin normalized to GAPDH at baseline and at 15 - 28 days of intermittent dosing was assayed using an immuno-chemiluminescence assays and results are presented as percentage of pre-dose levels (A) A reduction of more than 50% of p-cofilin levels were seen in 3/8 patients. (B) Phosphorylation of MLC2 was measured by IHC in pre- and post-treatment tumor specimens of patients treated with AT13148 showing reduction in phosphorylation in only 1/5 samples.

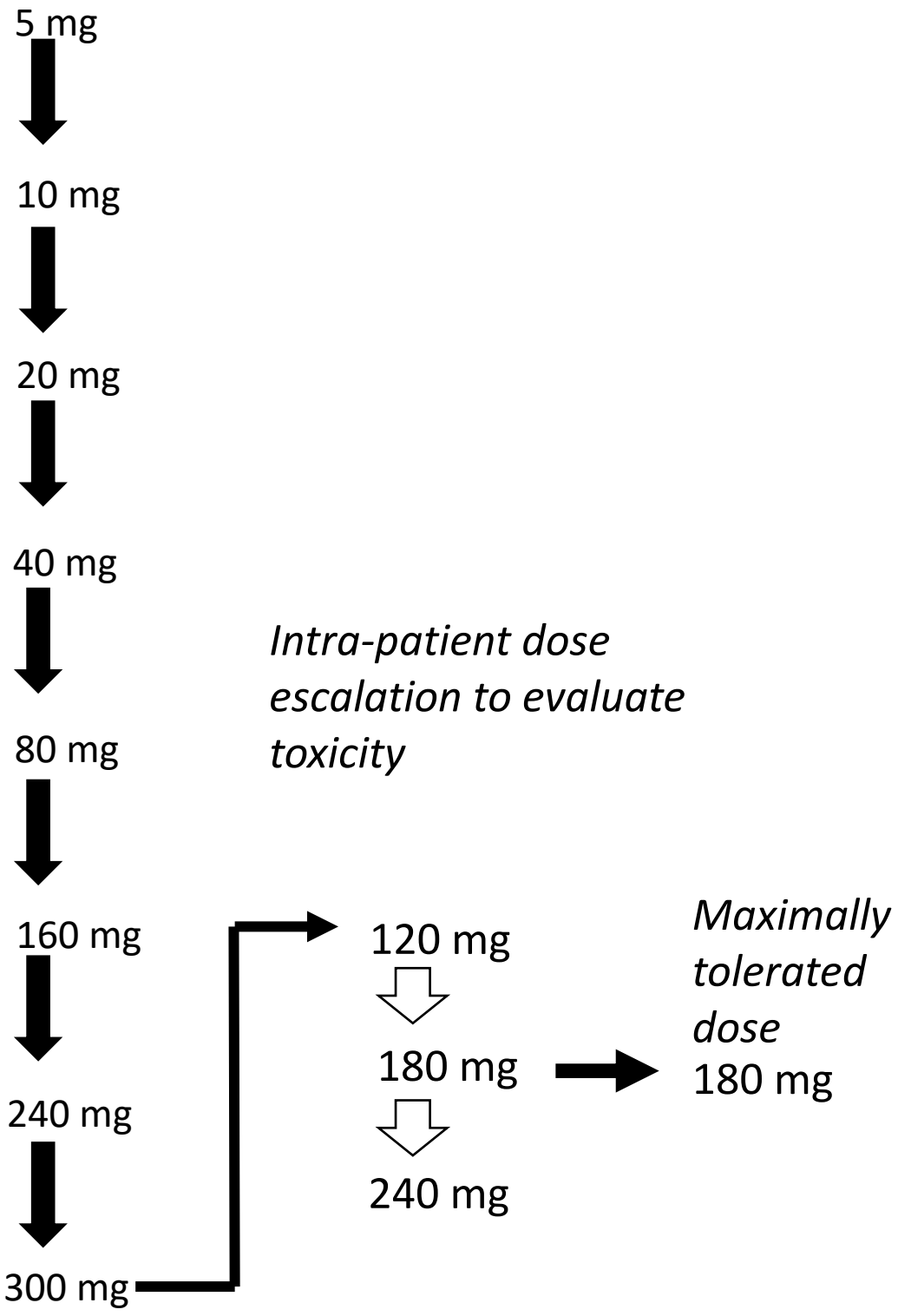
5 mg
10 mg
20 mg
40 mg
80 mg
160 mg
240 mg
300 mg
Intra-patient dose escalation to evaluate toxicity
120 mg
180 mg
240 mg
Maximally tolerated dose
180 mg

Figure 1

A

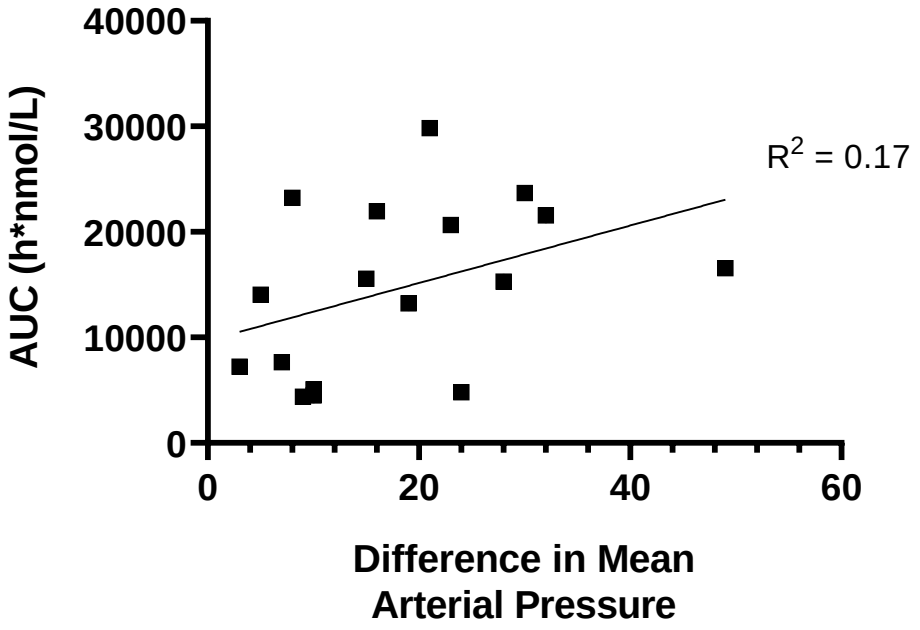
40000
30000
20000
10000
0
AUC (h*nmol/L)
R2 = 0.17
0
20
40
60
Difference in Mean
Arterial Pressure

B

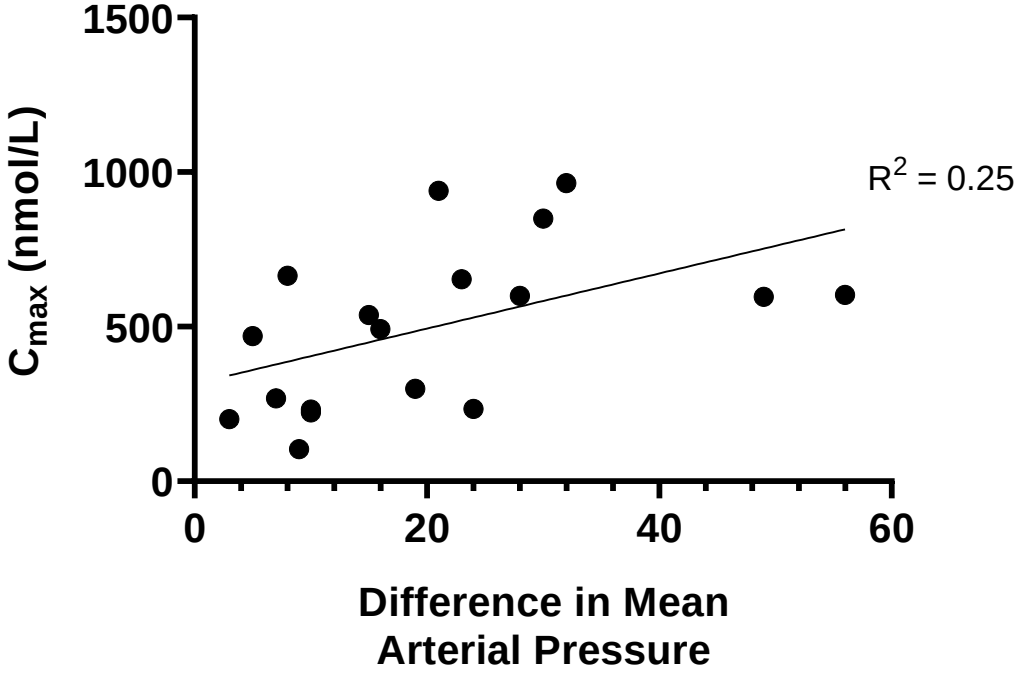
1500
1000
500
0
Cmax (nmol/L)
R2 = 0.25
0
20
40
60
Difference in Mean
Arterial Pressure

Figure 2

A

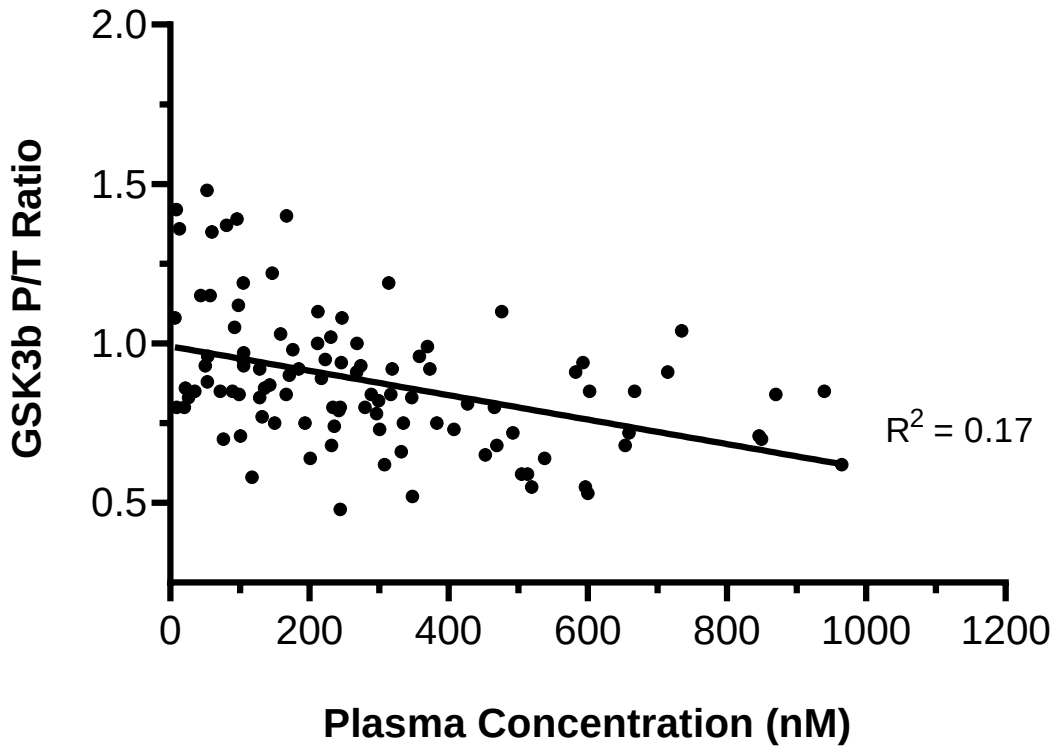
GSK3b P/T Ratio
2.0
1.5
1.0
0.5
0
200
400
600
800
1000
1200
Plasma Concentration (nM)
R2 = 0.17

B

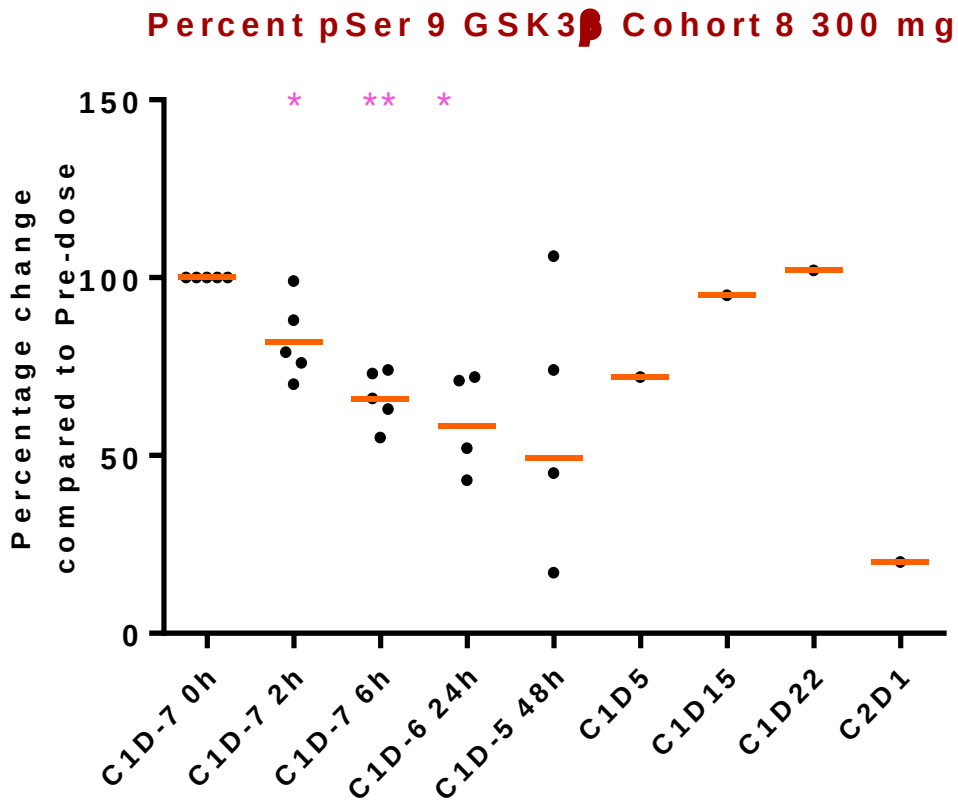
Percent pSer 9 GSK3β Cohort 8 300 mg
Percentage change compared to Pre-dose
150
100
50
0
*
**
*
C1D-7 0h
C1D-7 2h
C1D-7 6h
C1D-6 24h
C1D-5 48h
C1D5
C1D15
C1D22
C2D1

Figure 3

A

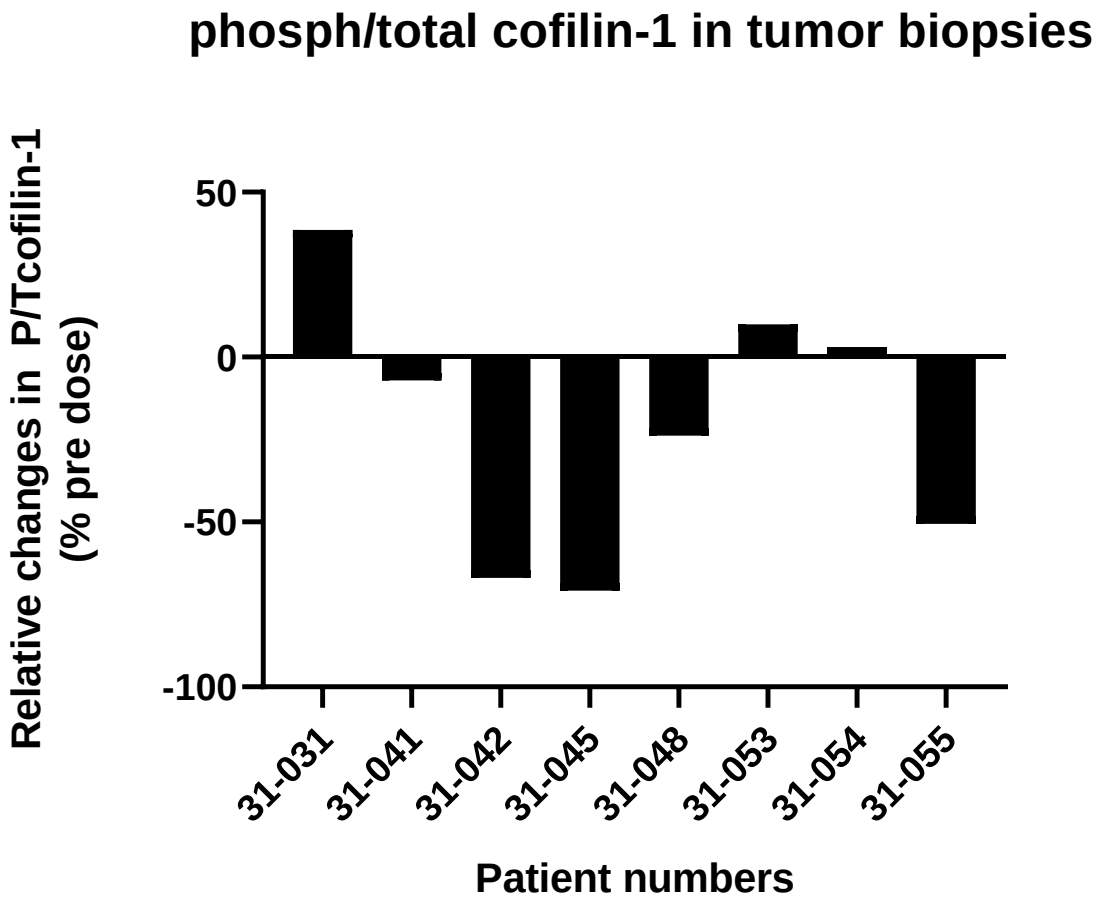
phosph/total cofilin-1 in tumor biopsies
Relative changes in P/Tcofilin-1 (% pre dose)
50
0
-50
-100
31-031
31-041
31-042
31-045
31-048
31-053
31-054
31-055
Patient numbers

B

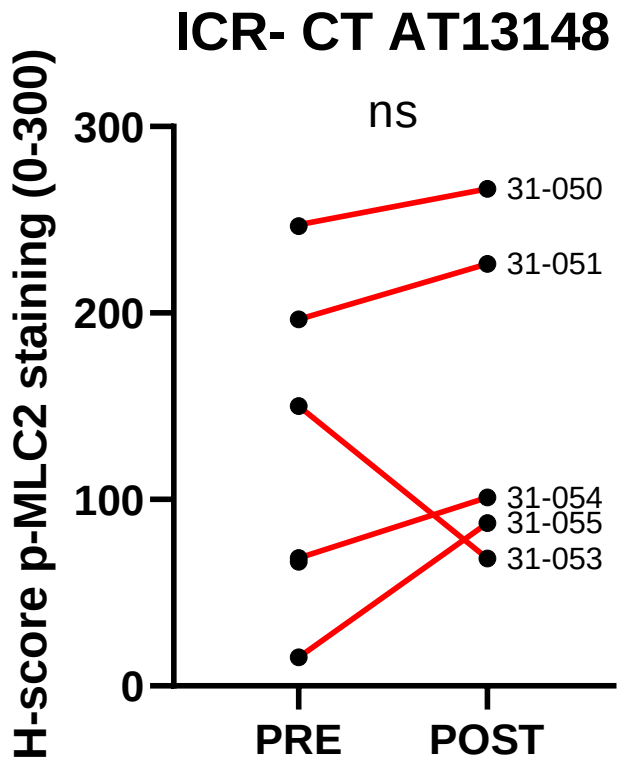
ICR- CT AT13148
ns
H-score p-MLC2 staining (0-300)
300
200
100
0
31-050
31-051
31-054
31-055
31-053
PRE
POST

Figure 4